Photoemission and optical processes in multialkali photocathodes

C. Ghosh*
Optoelectronics Section, Bhabha Atomic Research Center, Bombay 400085, India
(Received 17 May 1979)

Multialkali (Na_2KSb)Cs photocathodes have been studied in the range of photon energy of 1 to 6 eV by means of photoelectron spectroscopy, measurement of optical properties, and photoemissive quantum efficiency. The optical properties of these photocathodes are similar to the other alkali antimonides. The coincidence of the position of peaks and other similarities with the optical spectra of Na_2KSb supports the surface heterojunction hypothesis proposed by us earlier. The pseudopotential band-structure calculation by Klimin *et al.* on these materials has been used to identify the possible transitions taking place in the Brillouin zone corresponding to the observed structures in the optical spectra. From photoelectron spectroscopy the optical transitions appear to be of direct type, which puts this material in sharp contrast with other alkali antimonides, all of which showed the features of nondirect transitions. The threshold energy of electron-electron scattering for the photoexcited electrons have been found to be 2.3 eV which is more than twice the band gap above the conduction-band edge. The mean free path for this scattering has been found to be decreasing with increase of energy of the photogenerated electrons and, at an excitation energy of 6 eV, it is 43 Å. Apparently, the scattered electrons fall into a valley located 0.95 eV above the bottom of the conduction band. The increase of quantum efficiency with decrease of absorption after the onset of electron-electron scattering probably takes place due to generation of secondary electrons from the valence band due to scattering. Some of the peaks in the photoelectron spectra have been identified with the transitions predicted through the band-structure calculations.

INTRODUCTION

The multialkali (Na_2KSb)Cs photocathode has the highest quantum efficiency amongst the conventional alkali antimonide type of photocathodes.[1] It has a maximum quantum efficiency of about 0.3 electron/photon and the spectral response extends up to the near-infrared region; this is the most extensively used photocathode at present.

Investigations on this material have been carried out by a number of workers.[2-8] Spicer[2] measured the optical absorption coefficient in the range of photon energy of 1–3.5 eV. He used photoelectron spectroscopy[3] to find out the threshold of electron-electron scattering and mean free path. Sommer and McCarroll[4] determined the crystal structure of this material and attempted to explain the role of cesium. Dowman *et al.*[5] attempted to determine the structure and composition of the material and the surface. The electrical and other properties[6-9] were also studied.

In this paper a study of the optical properties through measurements of transmission and reflection and photoelectron energy spectra in a wide range of photon energy is presented. The optical properties of a photoemissive material are very important in determining the photoemission from it. The optical absorption in the alkali antimonide photoemitters shows some distinct characteristics.[10] The interband transitions for other alkali antimonide[11-14] and other photoemitters[13] were studied by photoelectron spectroscopy. The transitions were mostly found to be of a nondirect type in which the crystal momentum conservation is not an important selection rule. The nature of the optical transitions in this material was studied and has been found to be different. The photoelectron spectroscopy has been used to study other parameters such as the threshold for electron-electron scattering and the mean free path for such scattering. An attempt has been made to identify the various features available in optical properties and photoelectron spectroscopy with the calculated band structure of this material. The results would be important for further refinement of the electronic band-structure calculation of the alkali antimonide type of materials.

EXPERIMENTAL

The high-sensitivity multialkali photocathodes used for the measurements were prepared in the laboratory by means of a technique[6] in which the alkali metals and antimony were simultaneously evaporated at different stages at different temperatures. The ambient pressure during processing was 10^{-8} Torr obtained by a sputter ion and sorption pump system. The sensitivity of the photocathodes was around 250 μA/lm. The quantum efficiency has been measured by means of monochromator and thermopile combination in the region of wavelength of 400 nm and longer. A Schwartz Hilger FT 16 thermopile having a sensitivity of 27 μV/μW was used. At shorter wavelengths the tungsten- and hydrogen-lamp outputs were calibrated by using sodium salicylate phos-

phor having unity quantum efficiency. Freshly prepared phosphor films were used. For study of optical properties the photocathodes were prepared in a special type of "cell" which has two plane-parallel windows of polished silica.[15] These windows were sealed to the Pyrex cylindrical body of the cell by means of silver-chloride seal.[16] The antimony evaporator and alkali generators were placed outside and at the time of processing, the antimony evaporator was brought inside the cell by means of a magnet. After processing of the photocathode the cell was sealed from the vacuum system. The optical density and reflectance were measured, respectively, by a Cary 14 and Carl Zeiss M4QIII monochromator with a reflectance attachment.

For photoelectron spectroscopy the electronic system built was similar to that used by Traum and Smith.[17] The retarding voltage was modulated by a 33-cps sine wave of 70-mV peak-to-peak amplitude. Capacitive balance to reduce the effect of phototube capacitance was achieved by using a variable gain amplifier along with a balancing capacitor in the bridge. The ramp voltage was generated electronically and contributed little noise to the measurements. 50-cps (line) and 100-cps rejection filters were introduced along with a narrow-bandpass filter around 33 cps. A PAR 128A lock-in amplifier was used for the detection of the signal. The phototube was a spherical envelope and had an attached titanium sublimation pump which was started when the phototube was disconnected from the system during measurements. The vacuum in the phototube during measurements was about 1×10^{-11} Torr. The light was incident through a quartz window to the photocathode which was processed in a small glass disk coated with platinum. Monochromatic light was obtained through the Carl Zeiss M4QIII monochromator using tungsten and hydrogen lamps at appropriate energy ranges. The integral current was always less than 1×10^{-11} A. An energy resolution of about 100 mV was obtained with this system.

RESULTS AND DISCUSSIONS

Optical properties

Figure 1 is a plot of optical density versus wavelength as obtained from a Cary 14 spectrophotometer. The optical constants were calculated from reflectance (R) and transmittance (T) data using the following equations[18]:

$$R=\frac{(n-1)^2+k^2}{(n+1)^2+k^2},$$

$$T=(1-R)e^{-4\pi k(d/\lambda)},$$

$$\epsilon_1=n^2-k^2,\quad \epsilon_2=2nk.$$

Figure 2 shows the plot of the refractive index and extinction coefficient versus photon energy. The real (ϵ_1) and imaginary (ϵ_2) parts of the dielectric constant are also plotted as a function of photon energy in Fig. 3. Figure 4 is a plot of the optical transition strength as a function of photon energy.

The optical density spectrum of Fig. 1 is very similar to the spectra obtained by Ebina and Takahashi[10] for Na_2KSb. They also had observed two

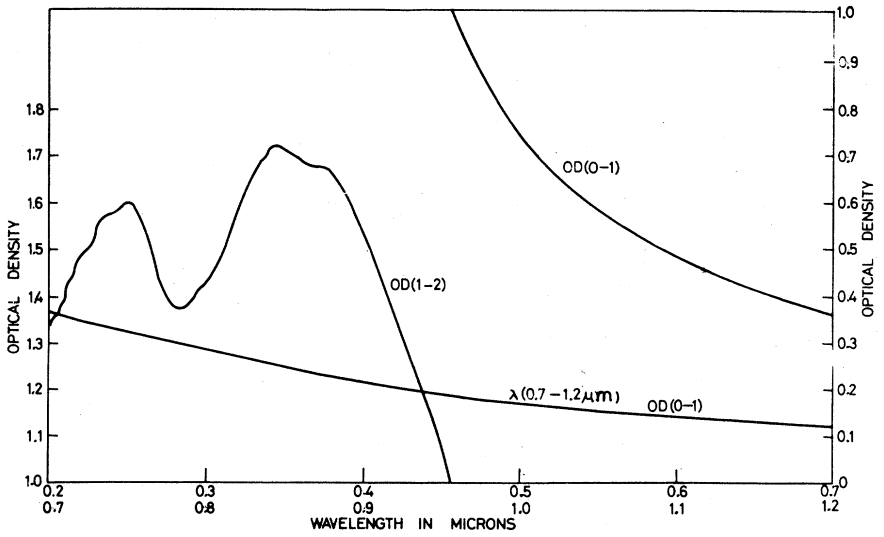

FIG. 1. Optical density versus wavelength spectrum for a multialkali photocathode as obtained by means of a Cary 14 spectrophotometer.

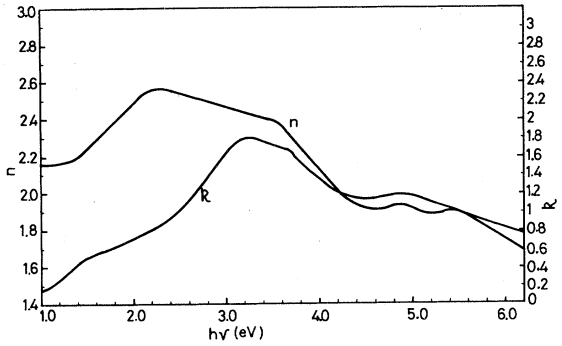

FIG. 2. Plot of refractive index (n) and extinction coefficient (k) versus photon energy for a multialkali photocathode.

absorption bands in the spectrum, each consisting of two peaks. The peaks in the lower-energy absorption band appeared between 3 and 4 eV while the peaks in the higher-energy absorption band appeared at energies of 4.85 and 5.25 eV for both high-sensitivity samples investigated. In the multialkali photocathode studied here the higher-energy peaks appear at 4.85 and 5.25 eV, exactly coinciding with that of Na_2KSb and the lower-energy ones appearing at 3.3 and 3.6 eV, similar to that in Na_2KSb. The ϵ_2 spectra, which closely correspond to the optical transition strength, are identical in these two photocathodes. This quantity has a very large peak at 3.3 eV followed by a smaller peak at 4.85 eV. Therefore, it is found that the position of absorption bands remains unchanged when the Na_2KSb is treated with cesium and antimony to prepare multialkali photocathodes. The optical absorption is a bulk property of a material and therefore this observation is in accordance with the model proposed by us for multialkali photocathodes.[6] Based on certain experimental observations it was proposed that the multialkali photocathode consists of bulk Na_2KSb with

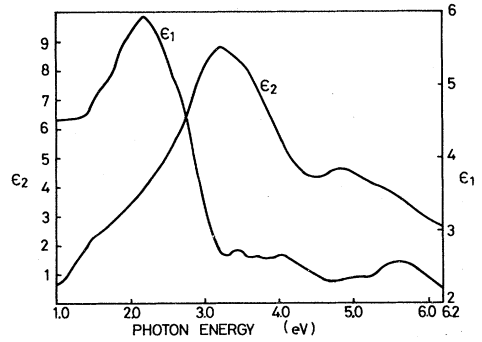

FIG. 3. Plot of real (ϵ_1) and imaginary (ϵ_2) parts of the dielectric constant with photon energy for a multialkali photocathode.

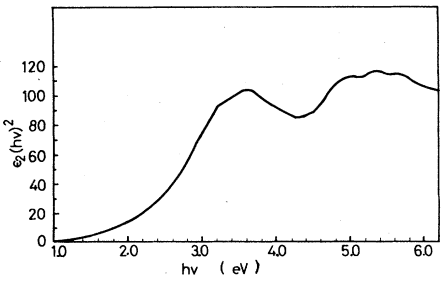

FIG. 4. Plot of optical transition strength $(h\nu)^2\epsilon_2$ as a function of photon energy for a multialkali photocathode.

a thin layer of K_2CsSb on it which forms a heterojunction and provides band bending at the surface.

The optical properties of alkali antimonide photocathodes of general chemical composition M_3Sb or $M_{3-x}N_xSb$, where M and N stand for alkali metals, appear to be similar in their gross shape.[10] It is characterized by two absorption bands at about the same energies and similar nature of ϵ_2, n, and k. In case of cubic alkali antimonide compounds, the sublattice of Sb and three sublattices of alkali atoms are all fcc. If the Sb lattice and two alkali atom lattices are taken into account, it results in the cubic antifluoride type of crystal structure.[19-22] Therefore the crystal structure of cubic alkali antimonide compounds can be considered to be made up of an antifluoride lattice and an alkali atom lattice consisting of the alkali atoms at the center of the cubes of the antifluoride. The optical properties of multialkali and some other alkali antimonides are similar to those obtained from semiconductor with antifluoride structure.[19,20]

The band structures of the alkali antimonide photocathodes have been calculated by pseudopotential[23] and empirical pseudopotential[24] methods. In the pseudopotential calculations, the Heine-Abarenkov model potential[25] was used to establish the qualitative nature of the band structure. In the empirical pseudopotential method, the crystal potential is constructed from the ionic potentials, the Fourier components of which are determined after appropriate interpolation to the new lattice period. The interpolation is done in such a way that the width of the forbidden zone of this compound is as close as possible to that experimentally observed. The calculated band structures of these compounds are very similar, and Fig. 5 shows the band structure of cubic K_3Sb, Na_2KSb, and K_2CsSb as obtained from pseudopotential calculations.[23]

The significant features of the band structure of these compounds are that the valence band is comprised of two narrow subbands separated by a large gap of about 6 eV. This implies that these

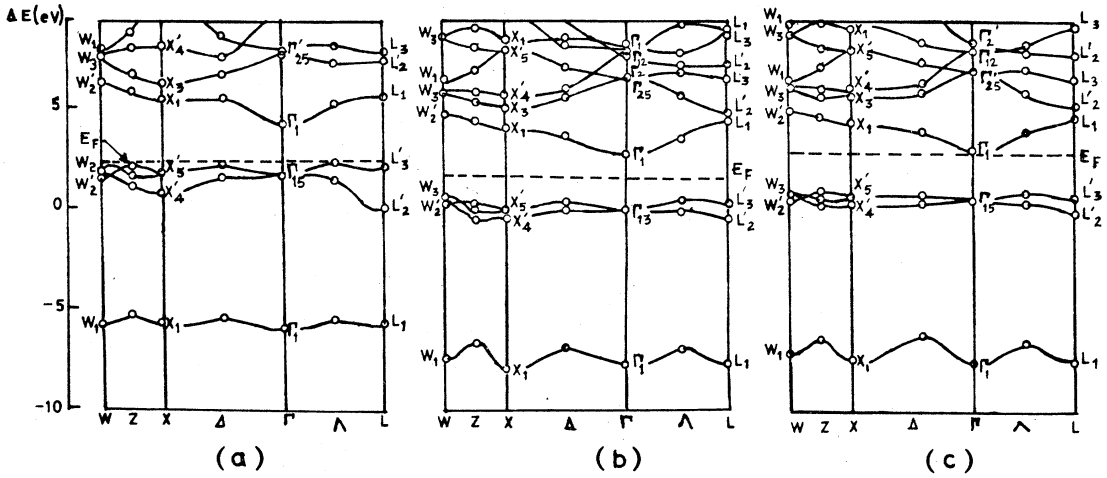

FIG. 5. Calculated band structure for cubic (a) Na_2KSb, (b) K_2CsSb, and (c) K_3Sb photocathodes (Ref. 23).

compounds have chemical bonds of highly ionic nature. The forbidden band is determined by the gap at a Γ point between Γ_{15} and Γ_1 in cubic K_3Sb, and Na_2KSb, between Γ_{6-} and Γ_{1+} in hexagonal K_3Sb, and between Γ_{2-} and Γ_{1+} in hexagonal Na_3Sb. In certain compounds such as cubic K_3Sb there is a forbidden gap in the conduction band between lower- and higher-energy subbands. If the spin-orbit interaction is taken into account, then the splitting of the levels of alkali atoms is an order of magnitude less than those of antimony atoms and hence can be neglected. It is found that for K_3Sb, owing to spin-orbit splitting, the top of the valence band at Γ would be split into two bands with an energy separation of 0.97 eV. The upper band would move upwards compared to the position of the top of the valence band obtained without taking into account spin-orbit splitting by an amount $\frac{1}{3}$ of the spin-orbit splitting, and the lower band would move down by $\frac{2}{3}$ of this splitting energy.

From an inspection of the band structure of Na_2KSb we can observe that the energy separation of the subbands of the valence band which are below the energy gap in the valence band are more than 8 eV from the bottom of the conduction band. Therefore, they cannot take part in optical transitions below an energy of about 8 eV. Hence, the optical properties in the present range of investigation should be due to the transitions from the top of the valence band to the conduction band. At the lower-energy end of the study of optical properties, the small bump in ϵ_2 and k spectra at 1.5 eV might be due to the transition between the lower of the spin-orbit-split Γ_{15} band with the bottom of the conduction band, the calculated energy separation between which appears to be about 1.7 eV. By observation of the optical-transition-strength spectrum (Fig. 4) one notes that it rises sharply above an energy of 2 eV. This is apparently due to the transitions in the Δ and Λ directions between the valence and the conduction bands. The first shoulder and peak in the optical-transition-strength spectrum at 3.3 and 3.6 eV are probably due to the transitions at both L and X points of the Brillouin zone. From the band-structure calculation, done without taking into account the spin-orbit splitting, strong transitions are indicated between L_3' and L_1 with the energy gap of 3.21 eV. At X point, the $X_5' - X_1$ gap is 3.16 eV, the $X_4' - X_1$ gap is 3.82 eV, and the $X_5' - X_3$ gap is 3.92 eV. The peak and the shoulder may be the results of these transitions. After 3.6 eV the optical transition strength falls down, probably because of the gap in the conduction band along Δ and Λ directions, so that only the Z direction is available for optical transitions. Again the optical transition strength starts rising after 4.5 eV of photon energy and there are three peaks at the energies of 4.85, 5.25, and 5.7 eV. The energy gap between Γ_{15} and Γ_{25} corresponds to an energy of 4.91 eV. The separation between the first and third peaks in optical transition strength at higher energy is 0.85 eV, while the calculated spin-orbit splitting of Γ_{15} is 0.97 eV. Therefore the first and the third peaks are probably due to transitions at Γ point from the top two valence subbands. The middle peak at 5.25 eV could be due to parallel bands in the Z direction making a strong contribution to the joint density of states.

Photoemission

Photoemission is considered to be a three-step process.[2] The first step is the absorption of

photons and consequent generation of photoelectrons. The second and third steps are the transport of the electrons from the point of generation to the surface and the escape from the surface. The photoexcitation of electrons from the valence to the conduction band would contribute to photoemission if the electrons are excited to the subbands above the vacuum level of the material. Therefore the photoemission would not necessarily be directly proportional to the absorption of the photons in the material because at a particular energy the contributions of the subbands below vacuum level to the joint density of states may become much larger than at other energies. To escape from the material, the photogenerated electrons have to move from the point of generation to the surface. During this transport from the point of generation to the surface the electrons might lose energy by scattering with the lattice atoms and defects and with the free and bound electrons. The scattering with the valence-band electrons has a threshold energy which is more than the band gap above the bottom of the conduction band. The electrons scattered from the valence band would gain more energy than band gap, and, if they gain more energy than the threshold for photoemission, they might escape and contribute to photoemission. The contribution of the secondary electrons generated in this manner to photoemission has so far not been identified, but in this material, as will be observed shortly, they apparently contribute to the photoemission. Figure 6 is the plot of quantum efficiency versus photon energy for the multialkali photocathode.

Photoelectron spectroscopy has been used earlier to investigate the alkali antimonide photocathodes.[11-14] From an examination of the photoelectron spectra of the compounds such as K_3Sb

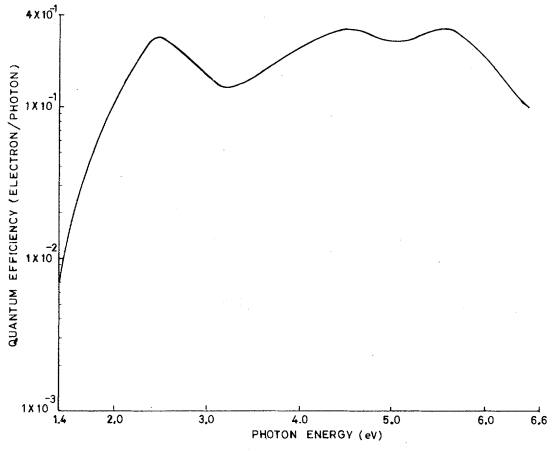

FIG. 6. Plot of quantum efficiency as a function of photon energy for a multialkali photocathode.

(Ref. 11), Cs_3Sb (Refs. 11–13), and K_2CsSb (Ref. 14) it was inferred that the optical transitions in these materials do not conserve the crystal momentum. In the case of so-called nondirect transitions, the structures in the photoelectron spectra, such as peak, shoulder, etc. arising out of the density of states in the conduction band would remain fixed on the energy scale if the photon energy is changed. However, if the structures are due to the density of states in the valence band, then those would be shifted by an energy equal to the change in photon energy. This is called the equal-increment rule.[26] We have also investigated the photoelectron spectra of these photocathodes mentioned above and found that the equal increment rule is obeyed with these. Figure 7 shows the energy distribution of the photoelectrons from multialkali photocathodes. Unlike other photocathodes, the equal-increment rule is not observed in this material. Therefore the transitions in this are probably of direct nature as is the case with most crystalline materials.

The large peak which is observed in the energy-distribution curves (EDC's) at higher energies is supposed to be due to the electrons which are slowed down due to scattering with valence-band electrons. This type of peak has been observed in all the alkali antimonide photocathodes investigated. The electron-electron scattering has a threshold energy which can be determined from the EDC's. The photon energy at which the slowed down electrons just appear is the threshold energy for this scattering process. In this material a shoulder due to the scattered electrons appears at a photon energy of 3.42 eV. The band gap of this material has been found to be 1.1 eV from photoconductivity experiment.[6] Therefore, the threshold energy would be 2.3 eV above the bottom of the conduction band, more than two times the band gap above the conduction-band edge. In good photoemitters the threshold energy for electron-electron scattering has been found to be more than twice the band gap above the conduction-band edge.[27] Spicer[3] also had determined the threshold for this scattering but he obtained a value of 4.1 eV above the valence-band edge. However, from the broadening of the EDC's before the shoulder is observable in his curves, it appears that the scattered electrons have appeared at much lower energies but were not detectable, probably due to the lower resolution of the instrument. Probably the scattered electrons fall into a valley in the conduction band and that is how the position of the peak due to the scattered electrons remains unchanged. As the electron affinity of this material is known to be 0.24 eV,[6] the position of this valley would be 0.95 eV above the bottom of the conduc-

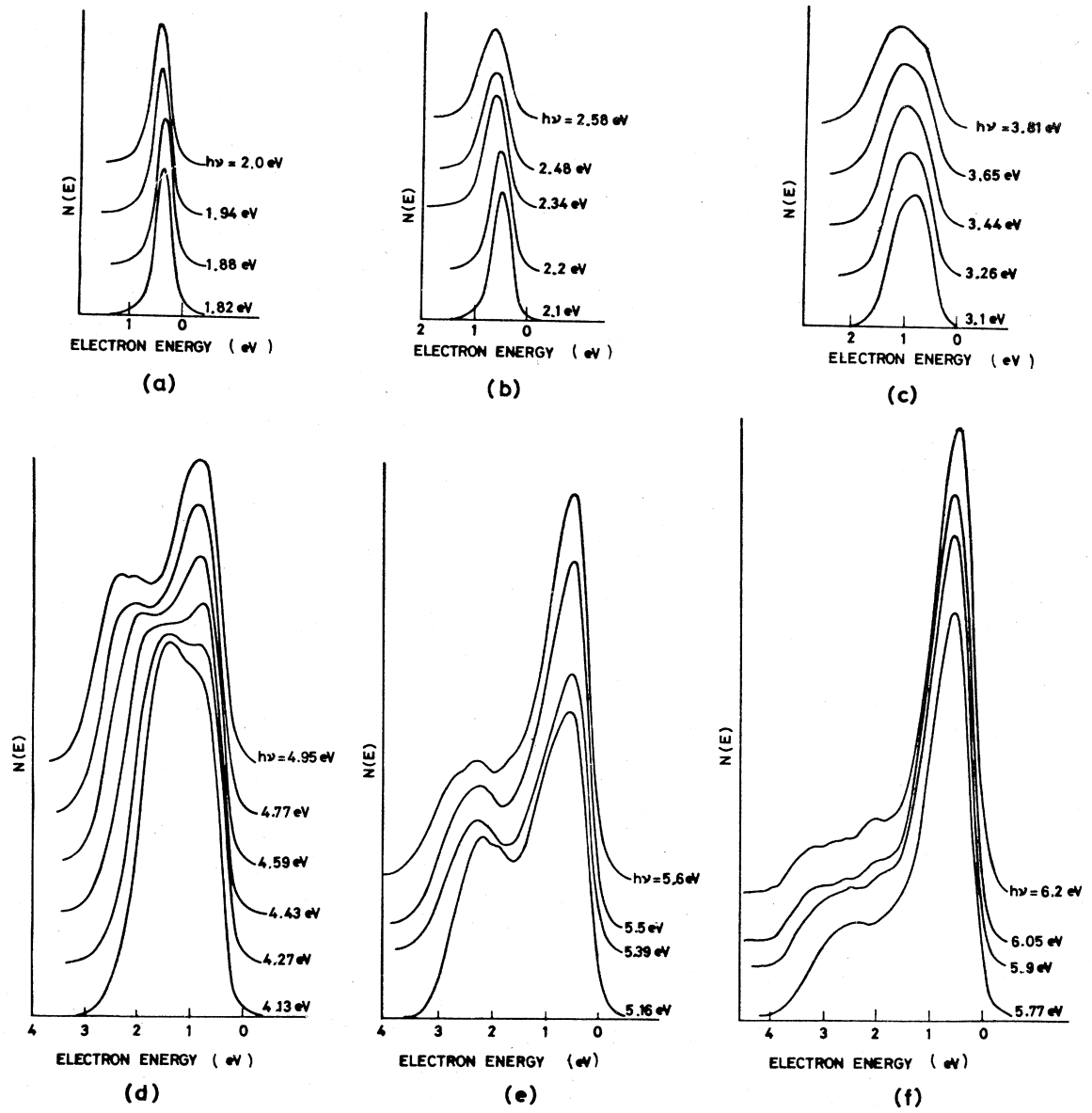

FIG. 7. Energy distribution of photoelectrons from multialkali photocathodes (a)–(f). The relative number of electrons $N(E)$ is plotted as a function of their kinetic energy. The incident photon energy is indicated along with each curve.

tion band. The position of this valley could be a good reference point for future band-structure calculations.

The loss of energy by the scattered electrons from the scattering event is 1.37 eV at the threshold for electron-electron scattering. Since the threshold energy for photoemission in the case of this photoemitter is 1.3 eV, the energy imparted to the valence-band electrons may cause the emission of these electrons provided they are from the top of the valence band. An inspection of the absorption index curve of Fig. 2 and the quantum efficiency plot of Fig. 6 shows that the quantum efficiency which was falling after a peak at an energy of 2.5 eV starts rising again from 3.4 eV although the absorption is decreasing. Even in the region of 3.6 to 4.5 eV when absorption falls down sharply, the quantum efficiency continues to rise rapidly. This is probably because of the secondary electrons created from the valence band because of electron-electron scattering. From an examination of the band structure the absorption in this region appears to be due to transitions in Δ and Λ directions and there are no nearby bands at higher energy, transitions to which would contribute to the increase in photoemission at this en-

ergy. Therefore the scattered electrons from the valence band might have produced the increase in photoemission at this energy as has been observed.

The mean free path for the electron-electron scattering could be found by measuring the relative number of low- (scattered) and high- (unscattered) energy electrons and the absorption coefficient at each energy by using the formula[3]

$$\ell(h\nu) = N_F / K(h\nu) N_S ,$$

where $\ell(h\nu)$ is the mean free path, N_F is the number of fast electrons, N_S is the number of slow electrons, and $K(h\nu)$ is the absorption coefficient. Figure 8 shows the variation of the mean free path with the energy of exciting photons. The mean free path changes very sharply in the lower-energy side compared to the higher-energy. Similar behavior of the mean free path was observed for multialkali photocathode by Spicer.[3] The magnitude of the mean free path in our multialkali photocathode is larger than reported by Spicer. For example, at 6 eV of photon energy he observed a mean free path of 15 Å, whereas in our case it is about 43 Å. He reports that at 5.7 eV of photon energy, the slow group contained about 75% of the total number of electrons. At the same energy the contribution to the slow group of electrons from our material is 80%. While this difference is not much, the difference in the value of the absorption coefficient brings about the difference in the mean free path in the two cases. The absorption coefficient, which is not reported in his work, must have been about three times higher than our value (5.4×10^5 cm^{-1}) at this energy.

The observation of the EDC at low energies when it contains only one peak shows that the position of the peak goes towards higher energies as the photon energy increases. But the position of the peak changes more slowly than the change of photo energy. The optical transitions in this region are predominantly along the Δ and Λ directions and the position of the peak moves along the subband in the conduction band. The position of the peak initially moves rapidly with change of photon energy because the slope of the band at the bottom of the conduction band is high around the Γ point. Then the rate of change of position with change of photon energy becomes much slower as it approaches X or L point and, after the X point, it again becomes faster as the transitions start taking place along the Z direction. In the Z direction, the transitions would give rise to two peaks at about an energy of 5 eV which has been observed. The separation of these two peaks is about 0.5 eV and is in reasonable agreement with the expected energy separation due to two parallel bands in the conduction band separated by an energy of about 0.7 eV. At still higher energies more peaks appear because higher-lying subbands in the conduction band are exposed and transitions take place to them.

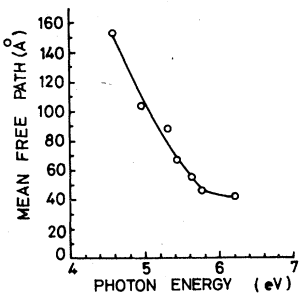

FIG. 8. Mean free path for electron-electron scattering versus photon energy for a multialkali photocathode.

CONCLUSIONS

The optical properties of multialkali antimonide are similar to those of other alkali antimonides in their gross shape. The coincidence of the position of the peaks and other similarities with the optical spectra of Na_2KSb supports the surface heterojunction hypothesis proposed earlier. With the band-structure calculations performed by Klimin *et al.* on these materials it is possible to identify the structures in the optical spectra with the possible transitions in the Brillouin zone of this material. From photoelectron spectroscopy the optical transitions have been found to be of direct type which puts this material in direct contrast with other alkali antimonides studied earlier. The threshold for electron-electron scattering of the photoexcited electrons has been found to be 2.3 eV, that is, more than twice the band gap above the bottom of the conduction band. The mean free path for this scattering has been found to be decreasing with increase of energy of the photogenerated electrons. At an energy of excitation of 6 eV the mean free path is 43 Å. The scattered electrons fall into a valley located 0.95 eV above the bottom of the conduction band. The increase of quantum efficiency with decrease of absorption when electron-electron scattering takes place is probably due to the generation of the secondary electrons from the valence band due to the scattering. Some of the peaks in the EDC's have been identified with the transitions in the Brillouin zone of this material.

ACKNOWLEDGMENTS

The author wishes to thank Mr. G. K. Bhide and Dr. B. P. Varma for their help and for many useful discussions. Thanks are also due Mr. D. N. Joshi and the departmental glass blowers for their technical assistance.

*Present address: Physics Department, Oregon State University, Corvallis, OR 97331.

[1]A. H. Sommer, Rev. Sci. Instrum. 26, 725 (1955).
[2]W. E. Spicer, Phys. Rev. 112, 114 (1958).
[3]W. E. Spicer, J. Phys. Chem. Solids 22, 365 (1961).
[4]W. H. McCarroll, R. J. Paff, and A. H. Sommer, J. Appl. Phys. 42, 569 (1971).
[5]A. A. Dowman, T. H. Jones, and A. H. Beck, J. Phys. D 8, 69 (1975).
[6]C. Ghosh and B. P. Varma, J. Appl. Phys. 49, 4549 (1978).
[7]C. Ghosh and B. P. Varma, J. Appl. Phys. 49, 4554 (1978).
[8]C. Ghosh and B. P. Varma, Thin Solid Films 46, 151 (1977).
[9]B. P. Varma and C. Ghosh, J. Phys. D 6, 628 (1973).
[10]A. Ebina and T. Takahashi, Phys. Rev. B 7, 4712 (1973).
[11]E. A. Taft and H. R. Philipp, Phys. Rev. 115, 1583 (1959).
[12]W. E. Spicer, Phys. Rev. Lett. 11, 243 (1963).
[13]F. Wootan, J. P. Hernandez, and W. E. Spicer, J. Appl. Phys. 44, 1112 (1973).
[14]R. Nathan and C. H. B. Mee, Phys. Status Solidi A 2, 67 (1970).
[15]C. Ghosh, Ph.D. thesis, Bombay University, 1976 (unpublished).
[16]B. P. Varma, Ph.D. thesis, London University, 1968 (unpublished).
[17]M. M. Traum and N. V. Smith, Phys. Rev. B 9, 1353 (1974).
[18]A. Vasicek, *Optics of Thin Films* (North-Holland, Amsterdam, 1960), p. 123.
[19]P. M. Lee, Phys. Rev. 135, A1110 (1964).
[20]N. O. Folland, Phys. Rev. 158, 764 (1967).
[21]M. Y. Au-Yang and M. L. Cohen, Phys. Rev. 178, 1358 (1969).
[22]W. J. Scouler, Phys. Rev. 178, 1353 (1969).
[23]A. A. Mostovskii, V. A. Chaldyshev, G. F. Karavaev, A. I. Klimin, and I. N. Ponomarenko, Izv. Akad. Nauk SSSR, Ser. Fiz. 38, 195 (1974).
[24]V. Heine and I. Abarenkov, Philos. Mag. 9, 451 (1964).
[25]A. A. Mostovskii, V. A. Chaldyshev, V. P. Kiselev, and A. I. Klimin, Izv. Akad. Nauk SSSR, Ser. Fiz. 40, 2490 (1976).
[26]F. Wooten, *Optical Properties of Solids* (Academic, New York, 1972), p. 154.
[27]A. H. Sommer and W. E. Spicer, in *Photoelectronic Materials and Devices*, edited by S. Larach (Van Nostrand, Princeton, 1965), p. 175.